Dislocation random walk under cyclic deformation

Atsushi Kubo [1,*] Emi Kawai,[1] Takashi Sumigawa [2] Hiroyuki Shima [3] and Yoshitaka Umeno[1]

[1]*Institute of Industrial Science, The University of Tokyo, 4-6-1 Komaba, Meguro-ku, Tokyo 153-8505, Japan*
[2]*Department of Energy Conversion Science, Graduate School of Energy Science, Kyoto University,*
Yoshida-Honmachi, Sakyo-ku, Kyoto 606-8501, Japan
[3]*Department of Environmental Sciences, University of Yamanashi, 4-4-37, Takeda, Kofu, Yamanashi 400-8510, Japan*

Dislocation motion under cyclic loading is of great interest from theoretical and practical viewpoints. In this paper, we develop a random walk model for the purpose of evaluating the diffusion coefficient of dislocation under cyclic loading condition. The dislocation behavior was modeled as a series of binomial stochastic processes (one-dimensional random walk), where dislocations are randomly driven by the external load. The probability distribution of dislocation motion and the diffusion coefficient per cycle were analytically derived from the random-walk description as a function of the loading condition and the microscopic material properties. The derived equation was validated by comparing the predicted diffusion coefficient with the molecular dynamics simulation result copper under cyclic deformation. As a result, we confirmed fairly good agreement between the random walk model and the molecular dynamics simulation results.

I. INTRODUCTION

Dislocation is one of the most typical lattice defects in crystalline materials and causes a strong effect on the mechanical properties by promoting plastic deformation [1–21]. Especially, dislocations play an important role in fatigue of metals, where dislocation microstructures are formed as a precursor of fatigue crack initiation [22–25], and thus it has been a key issue to control the dislocation motion for improving the reliability and lifetime of metal products. Thorough understanding of fatigue mechanism has been attempted from both the scientific and industrial viewpoints thus far. Experimental works have observed various types of microstructures resulting from cyclic deformation such as vein, persistent slip band (PSB), cell, labyrinth, etc., dependent on the deformation condition [26–30]. Dislocation patterning as a result of plastic deformation in crystalline materials has been an interesting scientific issue and subjected to a wide range of investigations from various aspects. In particular, a number of theoretical studies have been dedicated to this problem, which should be briefly reviewed here. One of the major successful approaches is construction of continuum dislocation theories that describe collective motion of dislocations under deformation. The development can be found in a series of papers by Groma, Zaiser, and coworkers, where they derived equations based on the motion of individual dislocations, applying methods from statistical physics [31–34]. Important fundamental rules of collective motion of dislocations and plasticity such as the Taylor hardening and the principle of similitude were explained by their theories [31], demonstrating that the dislocation patterning that arises during plastic deformation is dominated by long-range interactions between dislocations. The important role that

diffusional behavior of dislocations plays in the evolution of dislocation densities was highlighted and proved to affect the length scale selection of the dislocation density fluctuations [33]. Their deterministic and stochastic models of dislocation transport, constructed to discuss dislocation patterning, suggested the physical origin of dislocation patterns answering the long-term question, aka the energetic-vs-dynamic controversy [34]. Besides the continuum theory, collective motion of dislocations was also intensively investigated using discrete dislocation dynamics simulations [35–38]. Characteristic behaviors of dislocation systems behind plastic deformation, especially those as consequences of interaction with crystal defects, were well described in such models. For example, dislocation avalanches were found to exhibit different behaviors due to the effect of quenched pinning [35,36]. The discrete dislocation model elucidated dynamic hysteresis under cyclic loading [37] and strain-rate dependence of dislocation plasticity [38].

On the other hand, a model to reproduce dynamics of dislocation density distribution based on the reaction-diffusion theory has been proposed by Walgraef and Aifantis [39–42], which is hereafter called the WA model. In contrast to the aforementioned theoretical models, the WA model is a phenomenological one where the system is typically described as a continuum field of two types of dislocations called the immobile and mobile dislocations. The temporal evolution of their densities, $\rho_i(x, t)$ and $\rho_m(x, t)$, is given by the reaction-diffusion equations,

$$\frac{\partial \rho_i}{\partial t} = D_i \frac{\partial^2 \rho_i}{\partial x^2} + f(\rho_i, \rho_m), \tag{1}$$

$$\frac{\partial \rho_m}{\partial t} = D_m \frac{\partial^2 \rho_m}{\partial x^2} + g(\rho_i, \rho_m), \tag{2}$$

where D_i and D_m denote the diffusion coefficients of the immobile and mobile dislocations, respectively. The functions

*Corresponding author: kubo@ulab.iis.u-tokyo.ac.jp

f and *g* are the reaction terms, which represent nucleation and annihilation of dislocations and transform between immobile and mobile dislocations, etc. The one-dimensional periodic pattern (the ladder or wall structure in PSB) has been reproduced successfully by these equations, and the mathematical condition of microstructure formation has been derived by the linear stability analysis [43]. Several extended models have been proposed (e.g., three or more types of dislocations, two- or three-dimensional models) to describe more complex dislocation patterns [41,42,44,45].

In the mathematical models, it is of essential importance to determine proper ranges of the parameters. Recently, we have proposed an inductive (top-down) approach to estimate the diffusion and reaction parameters using the machine learning method [46]. Such a top-down approach is expected to provide a proper parameter set to be consistent with the experimental observation. Meanwhile, the diffusivity and reaction rate should be governed by the microscopic dynamics of individual dislocations, in principle. Thus, in addition to the top-down approach, the parameters should be determined or estimated by a bottom-up approach from the lower-scale mechanics on the basis of microscopic dislocation motion. A bottom-up derivation is important not only for parametrization but also for better understanding of fundamental physics behind the fatigue phenomenon. However, the diffusion and reaction properties have not been derived appropriately from the lower-scale mechanics because of the lack of theoretical models to bridge the scales of individual dislocations and continuum dislocation density field. In other words, it has not been discussed sufficiently thus far how to estimate the diffusion and reaction parameters in a theoretical way.

In this paper, we analytically derive the diffusion coefficient of dislocations under the cyclic loading condition, as part of an attempt to theoretically evaluate the diffusion and reaction parameters. Particularly, the mobile dislocations are investigated because they are expected to be diffused more and interact less strongly with each other than the immobile dislocations. The diffusion process is modeled as a random walk (RW), i.e., a series of binomial stochastic processes, and the diffusion coefficient is analytically obtained as a function of the loading condition and the microscopic material properties. The obtained equation is validated by molecular dynamics (MD) simulations, where we explicitly deal with the dislocation motion under cyclic deformation.

This paper is organized as follows. In Sec. II, we introduce the target material system and the preconditions to be discussed, and we formulate the RW model to evaluate the dislocation diffusion coefficient on the basis of the introduced preconditions. In Sec. III, we validate the RW model prediction by MD simulations. We conduct cyclic deformation simulations of copper crystal with dislocations, where we confirm the consistency between the RW model and the MD simulation. The results are further discussed in Sec. IV, compared with literature. Lastly, we conclude the paper in Sec. V.

II. DERIVATION OF RANDOM-WALK MODEL

A. Statement of preconditions

Figure 1 shows the schematic illustration of the system investigated in this paper, where the motion of a mobile dis-

location is modeled. We regard a loading cycle as a series of the elementary processes (i.e., a RW) undergone sequentially by the edge dislocations. The stochastic trials are done by assigning the elementary processes to the dislocations at random. Below, we clarify the conditions and assumptions to be considered.

(1) The system is two-dimensional. The dislocations in the system are straight and infinitely long. Only one slip system in a single crystal is taken into account. In other words, we assume a pure one-dimensional diffusion caused by slip on a single slip system. In addition, the effects of climbing motion or cross slip are regarded as negligible. The effect of the boundary condition is also negligible.

(2) The diffusion and reaction (interaction) contributions are explicitly separated, and a pure diffusion process is dealt with. This assumption is justified as a similar concept to the Langevin equation for a particle diffusing in solvent.

(3) Diffusion is mainly attributed to the external mechanical loading rather than thermal fluctuation. This assumption is justified by the following brief thought experiment: If thermal fluctuation was the main cause of diffusion, the dislocation microstructures would be formed spontaneously without any external loading, which is obviously contrary to the reality.

(4) The material behaves as a rigid perfectly plastic solid. In other words, the plastic strain is sufficiently larger than the elastic strain, and almost all the external strain is consumed as the plastic deformation.

(5) The dislocation driven by shear deformation keeps moving until being trapped by lattice defects (e.g., atomic vacancies, impurity atoms, etc.). Thus, a dislocation travels from one trapping site to a neighboring trapping site by the distance between two defects, *l* (hereafter referred to as the mean-free path). This process is regarded as the elementary process of the dislocation diffusion. Each cycle consists of a series of independent elementary processes. The direction of dislocation motion ($+l$ or $-l$) depends on the Burgers vector and the loading direction.

(6) The motion of a dislocation is affected by the point defects rather than other dislocations. This assumption is valid if the dislocation density is sufficiently low, i.e., in the case of the mobile dislocations.

(7) Each elementary process is assigned to dislocations at random with an equal probability.

B. Derivation of diffusion coefficient

Based on the preconditions above, we develop a specific model system for derivation of the diffusion coefficient, as shown in Fig. 2(a). We assume a two-dimensional body of rectangular-shaped single crystal with the edge lengths of L_x and L_y, including N dislocations, which undergo cyclic shear strain. Figure 2(b) shows schematically the relationship between the time and the applied shear strain in a single loading cycle. One cycle consists of four quarters; i.e., forward loading and unloading and backward loading and unloading, with the strain amplitude γ_{max}.

First, we focus on the first quarter of a cycle [forward loading, Q1 in Fig. 2(b)]; i.e., the process from the initial state (zero strain) to the maximum strain γ_{max}.
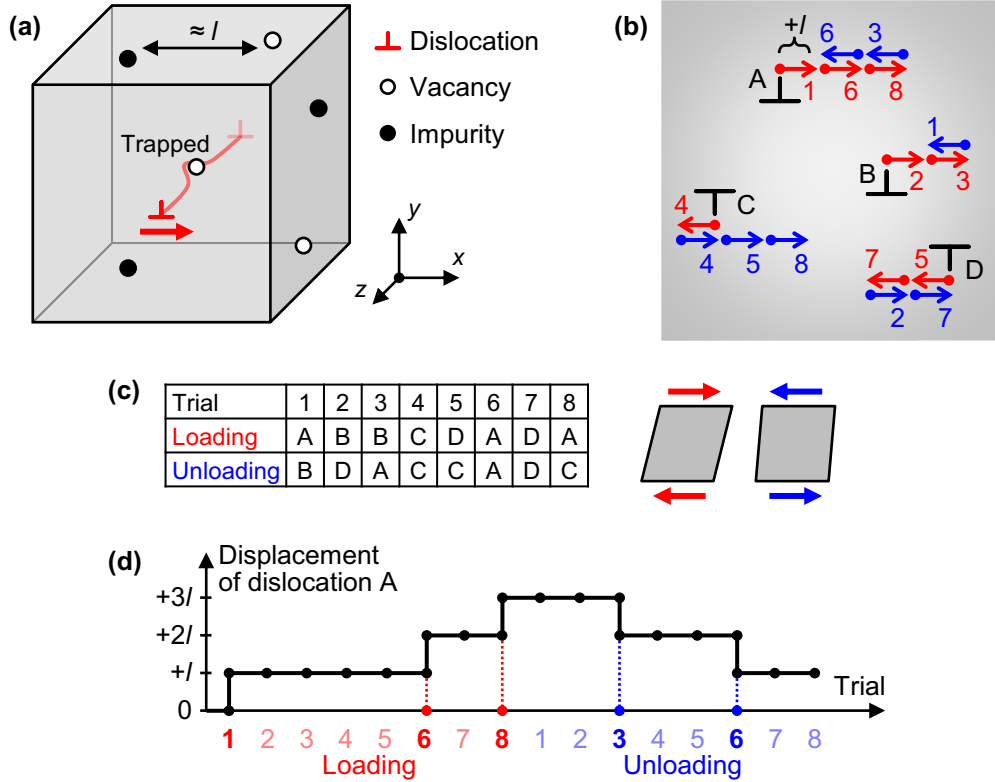
FIG. 1. Schematic illustrations of the system to be discussed. (a) Dislocations in a material are displaced by external shear load. Once a dislocation is driven, it moves until being trapped by lattice defects (vacancies, impurity atoms, etc.). The dislocation motion from one defect to the next defect is regarded as the elementary process. The mean-free path l can be approximated at the average distance between neighboring defects. (b) The plastic deformation process is regarded as a sequential series of the elementary processes assigned at random to the dislocations. As an example, we describe a system with four edge dislocations, A–D. The red and blue arrows represent the displacement of the dislocations in each elementary process under the loading and unloading conditions, respectively. The direction of the dislocation motion is dependent on the loading and unloading condition and the direction of the Burgers vector. (c) In the schematic, each of the loading and unloading processes consists of eight elementary processes to be assigned to the four dislocations. The number of trials is dependent on the amplitude of the applied strain. (d) Focusing on a specific dislocation (e.g., A), the displacement history can be visualized as a function of the trial number. Dislocation A is displaced by l to the right at trials 1, 6, and 8 at the loading stage, and to the left at trials 3 and 6 at the unloading stage (The activated trials are indicated with bold letters). While displacement of the dislocations should be zero on average after unloading, a nonzero residual displacement may be left, which is the origin of diffusion of dislocations in fatigue.

Dislocations move to release the applied shear strain. The total amount of displacement of all the dislocations, Δ, can be calculated geometrically as

$$\Delta = \frac{L_x L_y \gamma_{\max}}{b}, \tag{3}$$

where b denotes the length of the Burgers vector. The detail of derivation of this equation is shown in Appendix. The number of elementary processes in a quarter cycle, m, is simply given as the ratio of the total displacement Δ and the length of mean-free path l of the dislocation motion:

$$m = \frac{\Delta}{l} = \frac{L_x L_y \gamma_{\max}}{lb}. \tag{4}$$

Thus, m trials are assigned to N dislocations at random. Therefore, a dislocation is expected to move with probability $1/N$ or stay with probability $1 - 1/N$ in each elementary process:

$$p_{\mathrm{elem}}(\mathrm{move}) = \frac{1}{N}, \tag{5}$$

$$p_{\mathrm{elem}}(\mathrm{stay}) = 1 - \frac{1}{N}. \tag{6}$$

Hence, the quarter cycle is regarded as a RW with drift consisting of this elementary process. Since each dislocation undergoes this process m times in the quarter cycle Q1, the probability distribution of frequency (the number of times) to move, $p_{Q1}(k)$, is given as a binomial distribution

$$p_{Q1}(k) = {}_mC_k \left(\frac{1}{N} \right)^k \left(1 - \frac{1}{N} \right)^{m-k}, \tag{7}$$

where k represents the number of times that a (specific) dislocation moved ($k = 0, 1, 2, \ldots, m$). From the de Moivre-Laplace theorem [47], a binomial distribution can be approximated by a normal distribution; $p_{Q1}(k) \approx \mathcal{N}(\mu, \sigma^2)$, with the mean $\mu := \frac{m}{N}$ and the variance $\sigma^2 := \frac{m}{N}(1 - \frac{1}{N})$. The dislocation displacement ξ_{Q1} is given as $\xi_{Q1} = lk$, and thus we obtain the following probability distribution of dislocation displacement as $P_{Q1}(\xi_{Q1}) \approx \mathcal{N}(+l\mu, l^2\sigma^2)$. The distributions of displacement for other three quarters (Q2, Q3, and Q4) can be obtained in the same way as $P_{Q2}(\xi_{Q2}) = \mathcal{N}(-l\mu, l^2\sigma^2)$, $P_{Q3}(\xi_{Q3}) = \mathcal{N}(-l\mu, l^2\sigma^2)$, and $P_{Q4}(\xi_{Q4}) = \mathcal{N}(+l\mu, l^2\sigma^2)$. The residual displacement distribution after one cycle, ξ, can
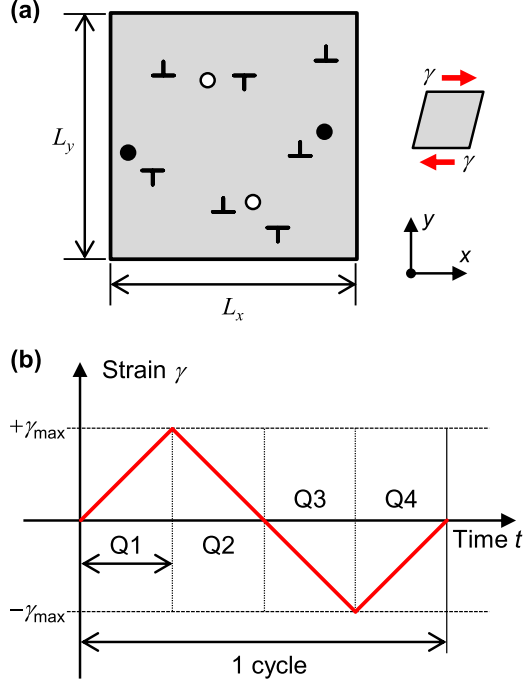
(a)

(b)

FIG. 2. (a) Geometry to be investigated for derivation of diffusion behavior. Since the interaction between dislocations is regarded as ignored, the position of dislocations can be set arbitrarily. (b) Schematic illustration of applied shear strain as a function of time in one cycle. Regions Q1–Q4 represent quarter cycles consisting of a single cycle: forward loading, forward unloading, backward loading, and backward unloading in the order.

be obtained as $\xi = \xi_{Q1} + \xi_{Q2} + \xi_{Q3} + \xi_{Q4}$. From the supposition of independence of each trial, the four distributions are additive, and the probability distribution of the displacement, $P_{cycle}(\xi)$, is obtained as $\mathcal{N}(0, 4l^2\sigma^2)$; i.e.,

$$P_{cycle}(\xi) = \frac{1}{\sqrt{2\pi\varsigma^2}} \exp\left(\frac{-\xi^2}{2\varsigma^2}\right), \qquad (8)$$

$$\varsigma^2 = 4l^2\sigma^2. \qquad (9)$$

Note that the nonzero drifts ($\pm l\mu$) in quarter cycles are completely canceled after the whole cycle. The diffusion coefficient per cycle, D, is directly obtained from the definition [48]

$$D = \frac{1}{2}\varsigma^2 = \frac{2\gamma_{max}l}{b\rho}\left(1 - \frac{1}{N}\right), \qquad (10)$$

where ρ is the number density of dislocation; $\rho := \frac{N}{L_x L_y}$. Especially, for sufficiently large systems ($N \to \infty$), we obtain

$$D \approx \frac{2\gamma_{max}l}{b\rho}. \qquad (11)$$

This is the main result of this paper. The diffusion coefficient is expressed as a functions of parameters whose physical meaning is clear. The strain amplitude γ_{max} and the length of the Burgers vector b are uniquely determined from the material and the test condition to examine. The mean-free path l and the dislocation density ρ are dependent on the microscopic structure of materials. In general, since point defects

TABLE I. Structural parameters and loading condition for MD simulations of cyclic loading deformation.

	L_x [nm]	L_y [nm]	N	γ_{max}	l [nm]	ρ [nm^{-2}]	Cycles
Case 1	19.9	20.1	2	0.01	4.98	0.0050	200
Case 2	19.9	20.1	2	0.02	4.98	0.0050	200
Case 3	19.9	20.1	2	0.05	4.98	0.0050	50
Case 4	19.9	20.1	2	0.01	9.95	0.0050	200
Case 5	19.9	20.1	2	0.02	9.95	0.0050	200
Case 6	19.9	20.1	2	0.05	9.95	0.0050	200
Case 7	15.3	15.1	2	0.02	5.10	0.0087	50
Case 8	30.7	30.2	2	0.02	5.11	0.0022	50
Case 9	19.9	40.3	4	0.02	4.98	0.0050	50
Case 10	19.9	40.3	4	0.02	9.95	0.0050	50

are distributed in three-dimensional space at random or in a certain order, it is difficult to calculate l directly and exactly for an arbitrary placement of defects. While one can easily guess from a simple dimensional analysis that the mean-free path is proportional to the cubic root of the point defect density, the exact form of equation is not established. In the MD simulation in the next section, the point defects are manually placed in an ordered way to uniquely determine l (see the next section for details). We also note that the obtained diffusion coefficient D is *not* per unit time but per one cycle, unlike usual diffusion phenomena.

It is interesting to consider the system with only one dislocation ($N = 1$) as an extreme case. In this case, no randomness is introduced to the deformation process because the dislocation motion is uniquely determined: The dislocation moves forward by a certain distance during loading and moves back by exactly the same distance during unloading. Thus, we expect $D = 0$ for $N = 1$, which is consistent with Eq. (10). Since the degree of freedom increases with increasing N, D is expected to rise with increasing N.

III. VALIDATION BY MOLECULAR DYNAMICS SIMULATION

A. Simulation setup

To verify Eqs. (10) and (11), we conduct MD simulations of cyclic loading, in which all the related parameters (γ_{max}, l, b, ρ, and N) are explicitly controlled. We dealt with edge dislocations in a face-centered cubic (FCC) copper (Cu) single crystal as a typical case of fatigue and examined ten cases (Cases 1–10) with different conditions as shown in Table I. We adopted the interatomic potential based on the embedded atom method developed by Mishin *et al.* [49]

Figure 3 shows an example of the simulation cells. We prepared a simulation cell of FCC Cu consisting of approximately 34 000–140 000 atoms with one or two pairs of edge dislocations (i.e., $N = 2$–4) in all cases. Since N is not sufficiently large, we verify Eq. (10) instead of Eq. (11). The most typical slip system {111}⟨110⟩ was considered as the active slip system. The lattice constant of Cu was evaluated as 0.363 nm at the temperature of 300 K (room temperature), and thus we obtained the length of the Burgers vector as $b = 0.257$ nm. The simulation cell size along the x and
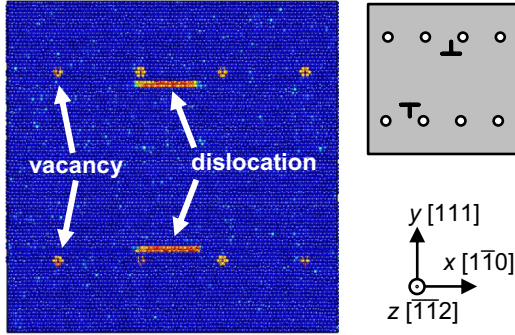
FIG. 3. Simulation cell of cyclic loading analysis for cases 1 and 2. Atoms are colored by the central symmetry parameter (CSP). The red atoms indicate the vacancies or stacking faults, and the blue atoms indicate the ideal FCC structure. Dislocations are split to two partial dislocations each, between which stacking fault regions are formed (indicated in red).

y axes was varied to examine the effect of the dislocation density ρ, while the size along the z axis was set equally for all cases as $L_z = 1.8$ nm. Thus, the dislocation density is evaluated as $\rho = N/L_x L_y$ and listed in Table I. In these simulation cells, the slip plane (111) is on the xz plane, and the slip direction [1$\bar{1}$0] is along the x axis. The periodic boundary condition was imposed on all three directions. Note that there are only two or four *independent* dislocations in the simulation cell, although the periodic boundary condition replicates the system infinitely. In this situation, the number of the dislocations is also regarded as $N = 2$ or 4 accordingly. In addition, atomic vacancies were introduced in the vicinities of the path of dislocation motion to explicitly determine the mean-free path l. Since the dislocations are trapped by vacancies, l is expected to be equal (or close) to the distance between vacancies. Note that, in the case of $N = 2$, the dislocations are kept nearly equivalent to each other through a cycle, and thus nearly ideal diffusion behavior is observed even though they interact with each other. We put two or four vacancies at equal distances along the x direction near the path of the dislocation motion, and then the mean-free path l was calculated by

dividing L_x by the number of vacancies. Cyclic shear strain γ_{zx} was applied to the simulation cell at the constant strain rate $d\gamma/dt = \pm 5 \times 10^{-5}$ ps^{-1} at the temperature of 300 K up to 50–200 cycles . The maximum shear strain (strain amplitude) γ_{max} was varied in the range of 0.01–0.05. All MD simulations were performed on the LAMMPS code [50].

B. Simulation results

Figure 4 shows the temporal evolution of the displacement of dislocations at cycle 1 in case 2, as an example. The position of dislocations was calculated as the center of mass of the stacking fault which was formed between the partial dislocations (see Fig. 3). Dislocations move continually, driven by the applied shear strain, and a nonzero residual displacement ξ is left after the cycle. Although unclear, the dislocation motion is discretized to some extent by being trapped in the vicinity of vacancies, which is consistent with the preconditions considered in Sec. II A. Also, after other cycles, some displacement is left as well, and the diffusion coefficient is evaluated from the variance of the probability distribution of the dislocation displacement. Note that the Peierls potential is sufficiently small compared to the kinetic energy (thermal fluctuation), and thus the effect of the Peierls potential is negligible. Figure 5 shows the probability distribution function of the displacement of dislocations after each cycle. The distribution (and thus the standard deviation ς) obtained by the MD simulation is in good agreement with that predicted by the RW model. Figure 6 compares the diffusion coefficients, D, evaluated by the MD simulations and the RW model. While the discrepancy in D is not very small (note $D \propto \varsigma^2$), it is still within an acceptable range for the practical use, i.e., to estimate the order of magnitude of D for the reaction-diffusion models.

The above results demonstrate the validity of the developed RW model despite the intensive simplification in the formulation.
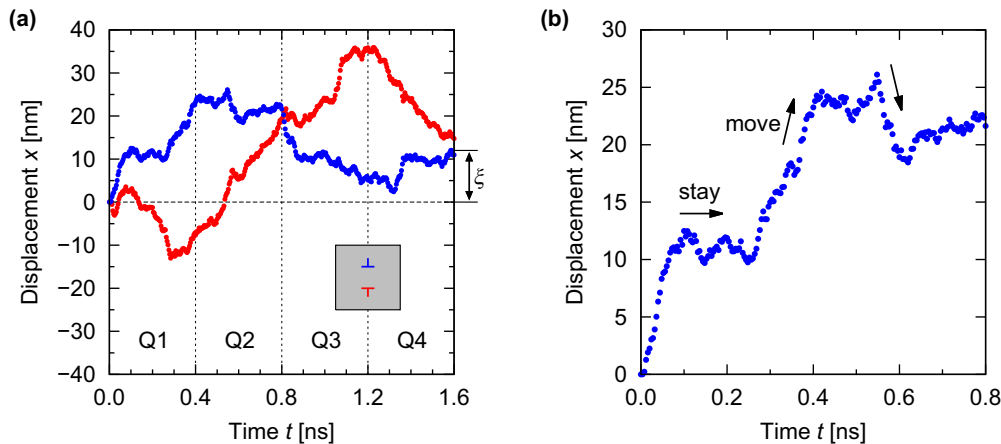

FIG. 4. Displacements of dislocations as a function of time at cycle 1 in case 2 for (a) entire cycle and (b) $t = 0-0.8$ ns. Two data series (blue and red) are two corresponding dislocations with opposite Burgers vectors (see inset). The residual displacement after cycle, ξ, is indicated by an arrow on the right of $t = 1.6$.
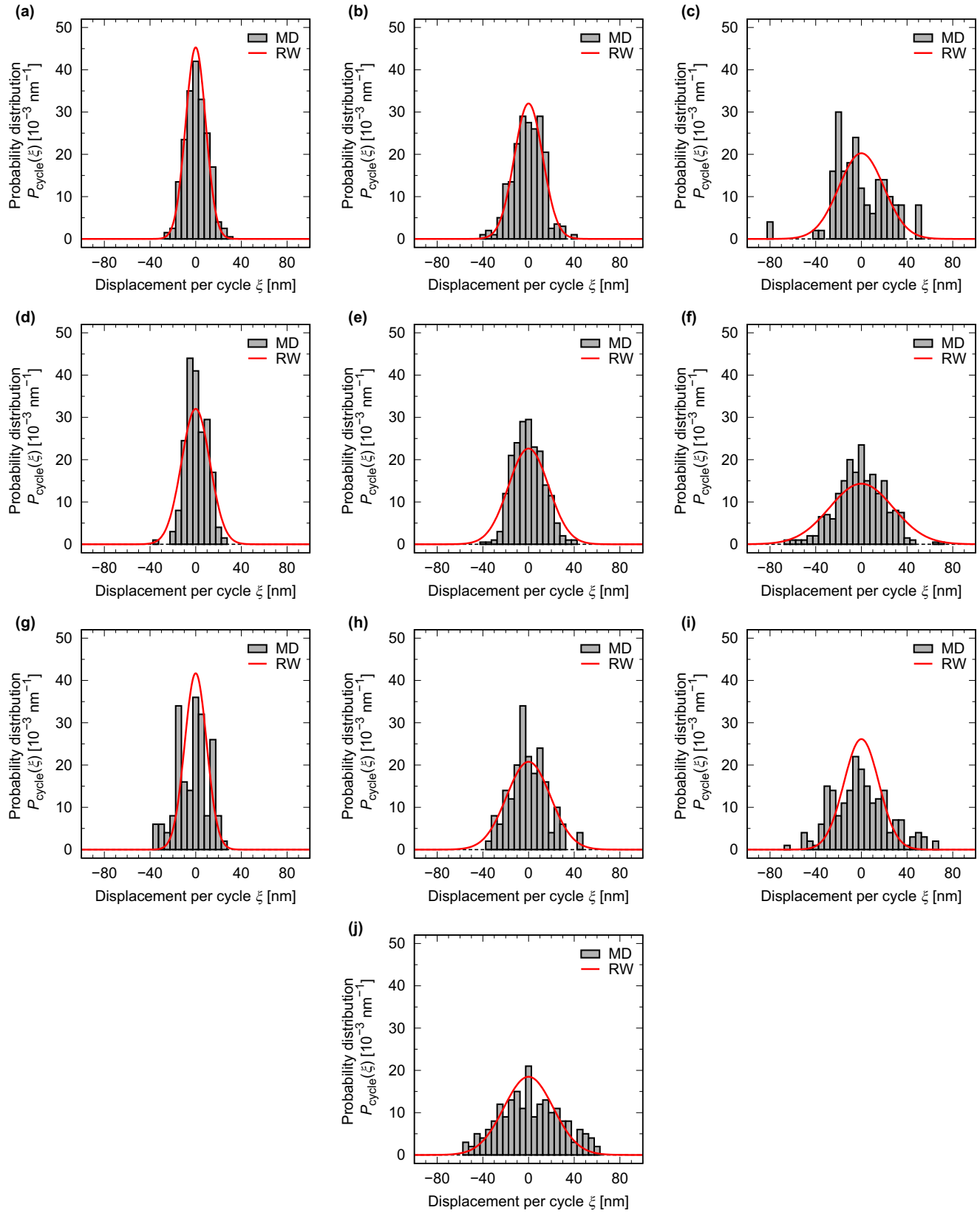
FIG. 5. Probability distribution of displacement of dislocations obtained by random walk (RW) model [Eqs. (8) and (9)] and molecular dynamics (MD) simulation for (a)–(i) cases 1-10 in the order.
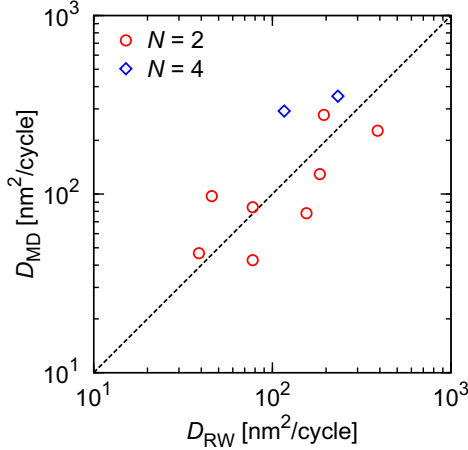
FIG. 6. Diffusion coefficients calculated by RW model and MD simulation.

IV. DISCUSSION

A. Comparison with literature

Indeed, Schiller and Walgraef [51] attempted to estimate the diffusion coefficient of the mobile dislocation. They calculated $D_m = v_m^2/2c$, where v_m denotes the effective velocity of the mobile dislocations and c is a parameter related to the reaction terms. The velocity was estimated from the Orowan equation [52]. In this way, however, it is difficult to explicitly take into account the effect of the test condition (especially, the strain amplitude γ_{max}, which characterizes the dislocation pattern). Another problem in the precedent evaluation [51] is that the time dependency is inevitably introduced into the equation, which is not consistent with the experimental fact that the fatigue behavior is insensitive to the strain rate [53–55].

On the other hand, the present model can naturally introduce the effect of the test condition (strain amplitude) and omit the time dependency. In other words, we established the diffusion model successfully without considering the complex dynamic effects (time-dependent motion) such as mobility, velocity, effective mass, etc. That was achieved by simply supposing that the diffusion of dislocations is mainly attributed to the plastic deformation by the cyclic loading. The parameters to be determined, i.e., the mean-free path l and the dislocation density ρ, are static properties, which can be estimated relatively easily.

B. Extensions of the model

1. Elastoplastic solids

It is worth noting that the material properties affect the diffusion coefficient in a quite simple way. Only the Burgers vector and the mean-free path, which is not an intrinsic property, appear in Eq. (11), but there is no effect of energetical character, i.e., the interatomic potential function, of the material. Although this absence of the potential function dependency is neither trivial nor intuitive, the reason can be clearly explained: That is attributed to the assumption of the rigid perfectly plastic solid, where the deformation behavior is uniquely determined regardless of the potential function

form. If the elastic deformation is not negligible compared with the strain amplitude, this assumption is needed to be modified accordingly. Our model can be easily extended from a rigid perfectly plastic solid (as formulated in Sec. II B) to an elastoplastic solid. For example, for an elastic perfectly plastic solid, the plastic strain exerted on the material, γ_{plast}, is given by subtracting the elastic strain γ_{elast} from the total strain γ; i.e., $\gamma_{plast} = \gamma - \gamma_{elast}$. Thus, we obtain the modified equation

$$D \approx \frac{2(\gamma_{max} - \gamma_{elast})l}{b\rho} \qquad (12)$$

from Eq. (11). It is another problem how to decompose the total strain into the elastic and plastic components. In the case of general elastoplastic materials, the detailed effects of the elastic and plastic contribution can be evaluated from the shear stress-strain relationship, which is obtained by MD simulations.

C. Dislocation dipole

The present RW model is valid only under the preconditions mentioned in Sec. II A, where the interaction between dislocations is sufficiently weak compared with the interaction between point defects and a dislocation. Such a condition is realized if the dislocation density is sufficiently small and dislocations can move nearly independently of each other. The *mobile* dislocations are expected to exist in such an environment, and thus our model is a good approximation to describe the behavior of a mobile dislocation. Meanwhile, it is expected to make several modifications to apply the model to the case of the *immobile* dislocations, i.e., dislocation dipoles. This is mainly because the motion of the immobile dislocations are strongly confined by the counterpart dislocation of the dislocation dipole, which breaks down the assumption of no interaction between dislocations (Sec. II A). It should also be noted that the length scale of dislocation motion is governed by the average distance between dislocations ($\approx \rho^{-1/2}$) [33,56] rather than the distance between the point defects l in the case of strongly interacting dislocations, and the nonlinear effect of ρ on the diffusion coefficient D is not negligible any longer. In such a situation, dislocation patterning is expected to obey a scaling law regarding $\rho^{-3/2}$. In addition, the diffusion motion of the immobile dislocations might be described as a barycentric motion of the dislocation pair. Nevertheless, the fundamental behavior of the diffusion can be modeled in a similar way to the present formulation, i.e., as a random assignment of the sequential elementary processes. The detailed formulation for the immobile dislocations and its validation will be left as a future work.

V. CONCLUSION

We aimed theoretical derivation of the diffusion properties of dislocations in crystalline materials undergoing cyclic deformation. By introducing drastic simplifications, we formulated the dislocation motion under cyclic loading as a one-dimensional RW, and analytically derived the diffusion coefficient per cycle as a function of loading condition (shear strain amplitude) and material properties (the Burgers vector, the dislocation density and the mean-free path). There, the

diffusive nature was attributed to the random assignment of displacement to individual dislocations. The validity of the derived equation was confirmed by the MD simulations of cyclic deformation of copper single crystal with dislocations. The diffusion coefficients obtained by the MD simulation were in fairly good agreement with the prediction by the RW model, indicating the validity of the proposed model. Our model enables semiquantitative estimation of the diffusion coefficient of dislocations, which can be applied to the larger-scale simulations such as the reaction-diffusion models.

In derivation of the diffusion coefficient in Sec. II B, we did not make any assumption for a specific material or a specific crystal structure. Therefore, the developed equations are applicable not only for metals but also for general materials, as long as the preconditions in Sec. II A are valid. For example, it is known that dislocation microstructures are formed in silicon by fatigue as well as metals [11,57]. In such functional materials, the fatigue microstructures may also influence the functional aspect. Moreover, recent experiments reported that various kinds of ionic crystals which have been recognized as brittle thus far (e.g., zinc sulfide [58], zinc oxide [59], etc,) can exhibit large plastic deformation under certain conditions. In those materials, the motion of dislocations is expected to attract more attention in the future for the mechanical and functional reliability design of the applications.

ACKNOWLEDGMENTS

APPENDIX: RELATIONSHIP BETWEEN APPLIED STRAIN AND DISPLACEMENT OF DISLOCATIONS

Here, we derive the relationship between applied shear strain and the total displacement of dislocations, i.e., Eq. (3), by demonstrating the equivalence between the motion of individual dislocations and the plastic strain in a homogenized body.
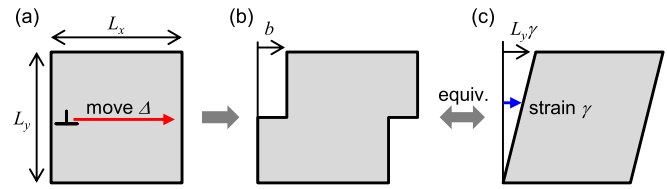

FIG. 7. Schematic illustration of system on thought experiment. Motion of a dislocation through the entire body (a) causes crystal slip as much as the length of the Burgers vector b (b), which is equivalent to the plastic deformation by shear strain $\gamma = L_y/b$ (c).

First, we conduct a thought experiment, supposing that an edge dislocation passes through the body (with the size of L_x and L_y) from left to right, as shown in Fig. 7(a). Then, the upper half of the body is displaced by the length of the Burgers vector, b [Fig. 7(b)]. Therefore, it is deduced that the displacement of a dislocation by L_x is equivalent to the plastic shear strain of b/L_y [Fig. 7(c)]:

$$\Delta = L_x \leftrightarrow \gamma = \frac{b}{L_y}. \quad (A1)$$

Next, we just note that the displacement of a dislocation Δ is proportional to the strain γ,

$$\Delta = C\gamma, \quad (A2)$$

where C is a constant coefficient, which is directly calculated from Eq. (A1) as

$$C = \frac{\Delta}{\gamma} = \frac{L_x L_y}{b}. \quad (A3)$$

Thus, we obtain Eq. (3) with $\gamma = \gamma_{\max}$.

We can discuss the system with two or more dislocations in the same way. As a conclusion, the plastic strain is simply dependent on the sum displacement of all the dislocations, regardless of the number of dislocations and their condition. The derived equation is equivalent to the time-integrated Orowan equation [52,60–62] from the initial state ($\gamma = 0$) to the maximal-strain state ($\gamma = \gamma_{\max}$).

[1] E. Orowan, Plasticity of crystals, Z. Phys. **89**, 605 (1934).

[2] M. Polanyi, Über eine Art Gitterstörung, die einen Kristall plastisch machen könnte, Z. Angew. Phys. **89**, 660 (1934).

[3] G. I. Taylor, The mechanism of plastic deformation of crystals. Part I.—Theoretical, Proc. R. Soc. London, Ser. A **145**, 362 (1934).

[4] G. I. Taylor, The mechanism of plastic deformation of crystals. Part II.—Comparison with observations, Proc. R. Soc. London, Ser. A **145**, 388 (1934).

[5] J. Hirth, A brief history of dislocation theory, Metall. Trans. A **16**, 2085 (1985).

[6] P. Rodriguez, Sixty years of dislocations, Bull. Mater. Sci. **19**, 857 (1996).

[7] D. Pashley, J. Menter, and G. Bassett, Observation of dislocations in metals by means of moiré patterns on electron micrographs, Nature (London) **179**, 752 (1957).

[8] Z. Basinski and S. Basinski, Dislocation distributions in deformed copper single crystals, Philos. Mag. **9**, 51 (1964).

[9] J. Steeds, Dislocation arrangement in copper single crystals as a function of strain, Proc. R. Soc. London A **292**, 343 (1966).

[10] K. Wessel and H. Alexander, On the mobility of partial dislocations in silicon, Philos. Mag. **35**, 1523 (1977).

[11] M. Legros, A. Jacques, and A. George, Cyclic deformation of silicon single crystals: Mechanical behaviour and dislocation arrangements, Mater. Sci. Eng., A **387-389**, 495 (2004).

[12] A. M. Minor, E. Lilleodden, M. Jin, E. Stach, D. Chrzan, and J. Morris, Room temperature dislocation plasticity in silicon, Philos. Mag. **85**, 323 (2005).

[13] V. Holland, Dislocations in polyethylene single crystals, J. Appl. Phys. **35**, 3235 (1964).

[14] J. Petermann and H. Gleiter, Direct observation of dislocations in polyethylene crystals, Philos. Mag. **25**, 813 (1972).

[15] A. Haziot, X. Rojas, A. D. Fefferman, J. R. Beamish, and S. Balibar, Giant plasticity of a quantum crystal, Phys. Rev. Lett. **110**, 035301 (2013).

[16] R. Pessoa, S. A. Vitiello, and M. de Koning, Dislocation mobility in a quantum crystal: The case of solid ^{4}He, Phys. Rev. Lett. **104**, 085301 (2010).

[17] O. V. Yazyev and S. G. Louie, Topological defects in graphene: Dislocations and grain boundaries, Phys. Rev. B **81**, 195420 (2010).

[18] J. H. Warner, E. R. Margine, M. Mukai, A. W. Robertson, F. Giustino, and A. I. Kirkland, Dislocation-driven deformations in graphene, Science **337**, 209 (2012).

[19] P. Schall, I. Cohen, D. A. Weitz, and F. Spaepen, Visualization of dislocation dynamics in colloidal crystals, Science **305**, 1944 (2004).

[20] P. Schall, I. Cohen, D. A. Weitz, and F. Spaepen, Visualizing dislocation nucleation by indenting colloidal crystals, Nature (London) **440**, 319 (2006).

[21] P. Schall, Laser diffraction microscopy, Rep. Prog. Phys. **72**, 076601 (2009).

[22] P. Neumann, Dislocation dynamics in fatigue, Phys. Scr. **T19B**, 537 (1987).

[23] S. Suresh, *Fatigue of Materials* (Cambridge University Press, Cambridge, 1998).

[24] P. Li, S. Li, Z. Wang, and Z. Zhang, Fundamental factors on formation mechanism of dislocation arrangements in cyclically deformed fcc single crystals, Prog. Mater. Sci. **56**, 328 (2011).

[25] P. Li, S. Li, Z. Wang, and Z. Zhang, Unified factor controlling the dislocation evolution of fatigued face-centered cubic crystals, Acta Mater. **129**, 98 (2017).

[26] N. Jin, Dislocation structures in fatigued copper single crystals oriented for double-slip, Phil. Mag. A **48**, L33 (1983).

[27] N. Jin and A. Winter, Dislocation structures in cyclically deformed [001] copper crystals, Acta Metall. **32**, 1173 (1984).

[28] U. Holzwarth and U. Essmann, Transformation of dislocation patterns in fatigued copper single crystals, Mater. Sci. Eng., A **164**, 206 (1993).

[29] P. Lukáš and L. Kunz, Role of persistent slip bands in fatigue, Philos. Mag. **84**, 317 (2004).

[30] C. Liu, M. Bassim, and D. You, Dislocation structures in fatigued polycrystalline copper, Acta Metall. Mater. **42**, 3695 (1994).

[31] M. Zaiser and S. Sandfeld, Scaling properties of dislocation simulations in the similitude regime, Modell. Simul. Mater. Sci. Eng. **22**, 065012 (2014).

[32] I. Groma, F. Csikor, and M. Zaiser, Spatial correlations and higher-order gradient terms in a continuum description of dislocation dynamics, Acta Mater. **51**, 1271 (2003).

[33] I. Groma, M. Zaiser, and P. D. Ispánovity, Dislocation patterning in a two-dimensional continuum theory of dislocations, Phys. Rev. B **93**, 214110 (2016).

[34] R. Wu, D. Tüzes, P. D. Ispánovity, I. Groma, T. Hochrainer, and M. Zaiser, Instability of dislocation fluxes in a single slip: Deterministic and stochastic models of dislocation patterning, Phys. Rev. B **98**, 054110 (2018).

[35] P. D. Ispánovity, L. Laurson, M. Zaiser, I. Groma, S. Zapperi, and M. J. Alava, Avalanches in 2D dislocation systems: Plastic yielding is not depinning, Phys. Rev. Lett. **112**, 235501 (2014).

[36] M. Ovaska, L. Laurson, and M. J. Alava, Quenched pinning and collective dislocation dynamics, Sci. Rep. **5**, 10580 (2015).

[37] L. Laurson and M. J. Alava, Dynamic hysteresis in cyclic deformation of crystalline solids, Phys. Rev. Lett. **109**, 155504 (2012).

[38] H. Fan, Q. Wang, J. A. El-Awady, D. Raabe, and M. Zaiser, Strain rate dependency of dislocation plasticity, Nat. Commun. **12**, 1845 (2021).

[39] D. Walgraef and E. C. Aifantis, Dislocation patterning in fatigued metals as a result of dynamical instabilities, J. Appl. Phys. **58**, 688 (1985).

[40] D. Walgraef and E. C. Aifantis, On the formation and stability of dislocation patterns—I: One-dimensional considerations, Int. J. Eng. Sci. **23**, 1351 (1985).

[41] D. Walgraef and E. C. Aifantis, On the formation and stability of dislocation patterns—II: Two-dimensional considerations, Int. J. Eng. Sci. **23**, 1359 (1985).

[42] D. Walgraef and E. C. Aifantis, On the formation and stability of dislocation patterns—III: Three-dimensional considerations, Int. J. Eng. Sci. **23**, 1365 (1985).

[43] K. G. Spiliotis, L. Russo, C. Siettos, and E. C. Aifantis, Analytical and numerical bifurcation analysis of dislocation pattern formation of the Walgraef-Aifantis model, Int. J. Non Linear Mech. **102**, 41 (2018).

[44] K. Differt and U. Essmann, Dynamical model of the wall structure in persistent slip bands of fatigued metals I. Dynamical model of edge dislocation walls, Mater. Sci. Eng., A **164**, 295 (1993).

[45] Y. SHIBUTANI, Mesoscopic dynamics on dislocation patterning in fatigued material by cellular automata, Mater. Sci. Res. Int. **48**, 258 (1999).

[46] Y. Umeno, E. Kawai, A. Kubo, H. Shima, and T. Sumigawa, Inductive determination of rate-reaction equation parameters for dislocation structure formation using artificial neural network, Materials **16**, 2108 (2023).

[47] A. Papoulis and S. U. Pillai, *Probability, Random Variables, and Stochastic Processes* (McGraw-Hill Europe, New York, 2002).

[48] A. Einstein, *Investigations on the Theory of the Brownian Movement* (Dover Publisher, New York, 1956).

[49] Y. Mishin, M. Mehl, D. Papaconstantopoulos, A. Voter, and J. Kress, Structural stability and lattice defects in copper: *Ab initio*, tight-binding, and embedded-atom calculations, Phys. Rev. B **63**, 224106 (2001).

[50] A. P. Thompson, H. M. Aktulga, R. Berger, D. S. Bolintineanu, W. M. Brown, P. S. Crozier, P. J. in't Veld, A. Kohlmeyer, S. G. Moore, T. D. Nguyen, M. J. Stevens, J. Tranchida, C. Trott, and S. J. Plimpton, LAMMPS —A flexible simulation tool for particle-based materials modeling at the atomic, meso, and continuum scales, Comput. Phys. Commun. **271**, 108171 (2022).

[51] C. Schiller and D. Walgraef, Numerical simulation of persistent slip band formation, Acta Metall. **36**, 563 (1988).

[52] E. Orowan, Problems of plastic gliding, Proc. Phys. Soc. **52**, 8 (1940).

[53] L. Buchinger, K. Kromp, and G. Schoeck, Ultrasonic fatigue of Cu-single crystals, Scr. Metall. **18**, 155 (1984).

[54] L. Buchinger, S. Stanzl, and C. Laird, Dislocation structures in copper single crystals fatigued at low amplitudes, Phil. Mag. A **50**, 275 (1985).

[55] C. Laird and L. Buchinger, Hardening behavior in fatigue, Metallurgical Transactions A **16**, 2201 (1985).

[56] D. Gómez-García, B. Devincre, and L. P. Kubin, Dislocation patterns and the similitude principle: 2.5D mesoscale simulations, Phys. Rev. Lett. **96**, 125503 (2006).

[57] A. George, A. Jacques, and M. Legros, Low-cycle fatigue in silicon: Comparison with fcc metals, Fatigue Fract. Eng. Mater. Struct. **30**, 41 (2007).

[58] Y. Oshima, A. Nakamura, and K. Matsunaga, Extraordinary plasticity of an inorganic semiconductor in darkness, Science **360**, 772 (2018).

[59] Y. Li, X. Fang, E. Tochigi, Y. Oshima, S. Hoshino, T. Tanaka, H. Oguri, S. Ogata, Y. Ikuhara, K. Matsunaga, and A. Nakamura, Shedding new light on the dislocation-mediated plasticity in wurtzite ZnO single crystals by photoindentation, J. Mater. Sci. Technol. **156**, 206 (2023).

[60] O. Ajaja, A dislocation network model of recovery-controlled creep, J. Mater. Sci. **21**, 3351 (1986).

[61] H. Mecking and K. Lücke, A new aspect of the theory of flow stress of metals, Scr. Metall. **4**, 427 (1970).

[62] S. Ojediran and O. Ajaja, The Bailey-Orowan equation, J. Mater. Sci. **23**, 4037 (1988).